ALMA Memo 543
Estimating Calibrator Counts at 250 GHz Using MAMBO Observations of Flat Spectrum Quasars

M.A. Holdaway and Chris Carilli
National Radio Astronomy Observatory
email: mholdawa@nrao.edu, ccarilli@nrao.edu

Axel Weiss
Max-Planck-Institute for Radioastronomy
email: aweiss@mpifr-bonn.mpg.de

Frank Bertoldi
University of Bonn
email: bertoldi@astro.uni-bonn.de

November 14, 2005

Abstract

We analyze the 250 GHz MAMBO fluxes of cm-selected bright, compact, flat spectrum quasars, match them with 8.4 GHz CLASS flux measurements, and derive a distribution for the spectral index between 8 GHz and 250 GHz. This spectral index distribution, when combined with Condon's 5 GHz flat spectrum source counts and the distribution of core fraction taken from the flat spectrum members of the 3CR[2] sample, provides us with an estimate of the source counts of bright, compact, flat spectrum quasars which will be available to ALMA at 250 GHz for various calibrations. Over the entire sky at 250 GHz, we find there should be about 28,000 quasars brighter than 10 mJy, 2230 quasars brighter than 100 mJy, and 70 quasars brighter than 1 Jy. The source count estimates in the current memo exceed the estimates of Holdaway and Owen (2005) at 250 GHz by 14% at 10 mJy, 33% at 100 mJy, and 55% at 1 Jy. The higher estimated counts as derived in this current work are a direct result of sources observed to have a very flat or even inverted spectral index between 8 and 250 GHz which were largely missing in Holdaway and Owen's spectral index distribution.

1 Introduction

ALMA's need for calibrators at 90 GHz for fast switching and pointing calibration measurements is well known. However, ALMA will also need calibrators at the higher frequencies for a variety of calibration observations:

- **fast switching instrumental calibration:** even if we are calibrating at 90 GHz, we will periodically need to find a source that is bright enough at both 90 GHz and the observing frequency in order to calibrate instrumental drifts which differ at the calibration and observation frequencies. We expect to do this about once every 5-10 minutes, and it should take about 5-20 s. Proximity to the target source is not a great concern as we do not need to connect the atmospheric phases, only the electronic phases, though distant sources will waste more time in slewing.

- **fast switching calibration at the observing frequency:** if we have a nearby calibrator which is bright at the target frequency, it may be more efficient to calibrate at the target frequency than to perform the two stage atmospheric/instrumental calibration involved in the usual description of fast switching. The results of the current work will help us study this tradeoff.

- **pointing offsets:** even though pointing will usually be performed at 90 GHz, ALMA's offset feed design requires that the pointing offsets among the various feeds be well calibrated, which will require occasional pointing calibration performed at all frequency bands.

- **aligning SD, ACA, and ALMA flux scales:** ALMA has a fairly loose 5% specification for the flux scale at sub-millimeter wavelengths. However, high quality imaging will require a much more accurate relative flux scale for the single dish, ACA, and ALMA-64 datasets. In order to accomplish this, we need to observe a common compact source which is bright enough to be easily and accurately detected by a single dish, the ACA, or ALMA.

- **focus:** we will have to focus at each frequency. At the high frequencies, the planets will be resolved to single dishes, so we will need to look for other smaller sources.

It would be very good if we had some idea of the numbers of bright sources available for calibrators, and hence, typical slew distances to sources of various strengths. The most comprehensive way to get source counts in a relatively unexplored part of observational phase space would be to do a large blind survey which detected hundreds of quasars. However, as beam sizes get smaller and sensitivity gets poorer with increasing frequency, and as we do not yet have an ALMA-class instrument, large-area source count experiments at high frequencies are not currently possible, though bolometer arrays may change this. However, it is possible to estimate the source counts given targeted flux measurements on cm-selected sources, as was done by Holdaway, Owen, and Rupen (1994, hereafter HOR). They generated a sample of 367 bright flat spectrum quasars (defined as $\alpha < 0.5$, $S_\nu \propto \nu^{-\alpha}$) selected from 8.4 GHz VLA Array core fluxes (Patnaik *et. al*, 1993), and observed them at 90 GHz with the NRAO 12m telescope. From the detections and upper limits at 90 GHz, and the 8.4 GHz core fluxes, HOR derived a distribution of spectral index between 8.4 GHz and 90 GHz, or $\alpha^{90}_{8.4}$. Flat spectrum source counts at 5 GHz (Condon, 1984), mainly determined from single dish measurements, were adjusted downward to estimate the contribution from just the core (the distribution of 5 GHz core fraction of these flat spectrum sources was derived from the properties of the flat spectrum members of the 3CR2 sample). After the 5 GHz flat spectrum counts were statistically adjusted to represent just the core emission, HOR then scaled the counts up to 90 GHz using the distribution of $\alpha^{90}_{8.4}$. We use these estimated 90 GHz flat spectrum counts

to estimate the density of ALMA fast switching phase calibrators on the sky. In addition, HOR observed 51 steep spectrum quasars with bright cores, and through the spectral index distribution between 8.4 GHz to 90 GHz of these cores, steep spectrum source counts at 5 GHz, and the distribution of core fraction of the steep spectrum members of the 3CR2 sample, were able to estimate that about 10% of the potential millimeter calibrators could be flat spectrum cores of steep spectrum sources.

Earlier this year, Holdaway and Owen (2005, ALMA Memo 520) dug deeper into the HOR work to extrapolate these source count estimates into the sub-millimeter. They decomposed the spectral index distribution into a population of sources which were still flat up to 90 GHz (19% of the sources) and a population of sources which had turned over to the optically thin spectral index between 8 GHz and 90 GHz. From the detailed shape of the spectral index distribution of the sources which had turned over, they inferred the distribution of break frequencies. If this distribution of break frequencies continued above 90 GHz, the remaining 19% of flat spectrum sources would all have turned over by 180 GHz. Using this model, the quasar source counts could be extrapolated to any ALMA observing band, though the uncertainty of this extrapolation increases with frequency above 90 GHz.

One of the motivations of the model of Holdaway and Owen was the unexpected discovery of three flat spectrum non-thermal sources brighter than 10 mJy at 250 GHz, discovered over about a square degree by MAMBO (Voss et al., 2005). Those three sources were significantly more than the Holdaway and Owen count estimates indicate there should be.

In the present memo, we use 250 GHz observations of these same cm-selected bright, flat spectrum quasars to better estimate the quasar (ie, calibrator) source counts at 250 GHz and compare these numbers to the Holdaway and Owen extrapolations.

2 Our Model for Source Counts at 250 GHz

We wrote software for manipulating the source counts in AIPS++/glish. This software is based on a fine grid in source flux S ranging from a very low flux (typically 1 mJy) up to 100 Jy, with resolution equal to the minimum flux, and differential source counts for each flux bin. For computational purposes, we select some number of total sources (such as 1e+6). The total number of sources plus an initial specification of 5 GHz flat spectrum source counts (Condon, 1984) imply a geometrical sky area. The input source counts can be differential or integral, and we convert to differential for our computation. Condon's 5 GHz flat spectrum source counts are differential. The differential source counts are interpolated onto each cell of our internal fine flux grid. The differential source counts per bin is merely a mathematical construct, and can be fractional. Indeed, in the very fine bins at high flux levels, there will be much less than one source per bin unless a huge number of sources (and hence a non-physical sky area) are used. There will be some problems at the very edges of the source count grid, but those problems tend to vanish as the counts go to zero at the high flux end, and the two effects we deal with, core fraction distribution and spectral index distribution, tend to push sources to lower flux, or off the lower end of the scale, though the spectral index distribution has some inverted sources with $\alpha = -0.4$ which can have 250 GHz fluxes $\simeq$5 times brighter than the 5 GHz fluxes. So, in order to make the calculations accurate at 10 mJy, we make the grid go down to 1 mJy.

2.1 Core Fraction Distribution

Flat spectrum radio sources will be dominated by the optically thick flat spectrum core emission, but at low frequencies like 5 GHz each source will be contaminated by varying amounts of steep spectrum extended emission. It is only the flat spectrum flux in the core which will be relevant for millimeter calibration sources, so the first processing step is to estimate the core fraction distribution and to scale down the flat spectrum source counts considering that distribution. The core fraction distribution is derived from the core flux divided by the total flux at 5 GHz for every quasar in the 3CR2 catalog, and that distribution is shown in Figure 1. About half the sources reside in the uppermost bin (95-100% of the source's flux is in the core), so accounting for the core fraction will make a small reduction in the 5 GHz source counts.

The core fraction distribution affects the source count grid in a simple manner: the number of sources in a given flux bin are spread out to lower fluxes by the core fraction distribution. Half of the sources don't budge (ie, keep 95-100% of their flux), the other half are sent to populate lower flux bins. However, the way the source counts go, there should be more and more sources in each lower flux bin, and spreading out the sources in a given flux bin to lower flux bins will therefore reduce the source counts.

2.2 250 GHz Data

The sample of bright, compact, flat spectrum sources that formed the basis of our earlier millimeter quasar count estimates (Patnaik, 1993) has also been observed at 250 GHz as pointing sources for IRAM. Data have been compiled from the IRAM database for pool observations. Measurements consist of pointing scans (cross scans) as well as pointed on-off observations of QSOs obtained with the MAMBO-1 (37-channel) and MAMBO-2 (117-channel) bolometer cameras at the IRAM 30m telescope during pool observing sessions between 2002 and 2005. Pointing scans with offsets larger than 3" or with noticeable flux differences between azimuth and elevation scan directions have been omitted. The rms of individual measurements varies strongly depending mainly on the weather conditions during the observations. Typical 3 sigma statistical noise levels are about 20mJy. Sources below 100mJy flux density have typically been observed only once (and hence do not provide any information on variability at 250 GHz). Bright (>1Jy) sources, which are frequently used for pointing and focusing, routinely have 25 to 100 flux measurements leading to a lower systematic uncertainly of these flux determinations. However, the intrinsic variability of these sources will be larger than the statistical noise. Whenever a source has been observed more than once, we have averaged all flux measurements.

A histogram of percent variability at 250 GHz (defined as $100 * \sigma_S / < S >$) is shown in Figure 2. This distribution is not used in our analysis, but is useful in thinking about tracking calibrators at high frequency. Note that of these sources which have been observed more than once, 110 of them had flat spectral index between 8.4 and 250 GHz and 19 of them had turned over to steep spectral index. This is due to a selection effect: most sources with spectra which turned over before 250 GHz were weak enough at 250 GHz so as not to be of interest for pointing observations and were not observed more than once. The distribution of variability for flat and steep spectrum sources is not dissimilar, and a Kolmogorov-Smirnov test indicates that there is a 22% probability that the variability distributions are the same for flat and steep spectrum objects. Remember, at centimeter wavelengths, ALL of these sources are flat spectrum.

2.3 Spectral Index Distribution

In all, there were 438 sources in the 250 GHz MAMBO database which were used (or attempted to be used) for pointing sources. These sources came from different surveys: most are Patnaik sources (cm-selected flat spectrum, compact, core-dominated sources), some are VLA calibrators (a heterogeneous sample), and a few are from somewhere else altogether. Of the 438 MAMBO pointing sources, 313 also have 8.4 GHz fluxes measured by the CLASS survey (Myers *et al.*, 2003; CLASS is a homogeneous sample of cm-selected compact flat spectrum sources like Patnaik's sample, and includes only northern sources). Therefore, sources with 250 GHz fluxes from MAMBO which also have 8.4 GHz measurements in CLASS represent a fairly homogeneous sample. We include the 8 GHz and 250 GHz fluxes of those 313 northern bright compact quasars in Tables 1-11. If multiple observational epochs were available, we averaged the fluxes. The noise level in the 8.4 GHz fluxes is under 1 mJy, but the flux scale errors of order 1% will usually dominate The 250 GHz fluxes have variable noise, as they have been observed between 1 and 100 times. When multiple observations were available, we averaged all the data. The 3 sigma detection limit for single observations at 250 GHz is about 20 mJy, so sources with 250 GHz fluxes lower than 20 mJy are considered non-detections. The spectral index is calculated as

$$-\log(S_{250}/S_{8.4})/\log(250/8.4),$$

and non-detections at 250 GHz have lower limits of the spectral index calculated with $S_{250} =$ 20 mJy.

The 250 GHz MAMBO pointing database included 10 northern sources which were not in the CLASS survey. Seven of these 10 northern sources which are not in the CLASS survey are in the VLA calibrator list, and five of those seven turn out to be steep spectrum sources. As the CLASS list contains sources known to be compact flat spectrum objects, we only used MAMBO sources which were also in the CLASS list. The remaining 115 MAMBO sources which were not in the CLASS survey were southern sources, which we omit from our analysis because it is difficult to obtain 8.4 GHz fluxes for the flat spectrum members of this group in a systematic way short of observing them.

Of the 313 sources included here, only 31 (10%) were below the 3 sigma 20 mJy detection limit at 250 GHz. Surprisingly, 198 (63%) remain "flat spectrum" up to 250 GHz, as defined by $\alpha < 0.5$. Only 28 sources (9%) appear to be inverted (brighter at 250 GHz than at 8.4 GHz). Some 25 sources (8%) fall off more steeply than the optically thin spectral index of 0.8.

Most of the inverted sources are modestly inverted, with spectral index ranging from -0.1 to 0. Originally, we were just looking at the average of the last five flux measurements at 250 GHz. However, some sources, notably J2253+161 (aka 3C454.3) and J0010+110 (aka III Zw 002), are currently experiencing flaring episodes. The flares start out at high frequency where the jet becomes optically thin closer to the central engine. At low frequency, the transition from optically thick to optically thin synchrotron emission occurs much further out along the jet, so a source flaring at high frequency will initially show no signs of flaring at low frequency, which could lead to a highly inverted spectrum. Furthermore, just a few sources with highly inverted spectra can have a profound affect on the estimated source counts at 250 GHz as they open up a gateway for a small fraction of the abundant low flux sources at 5 GHz to rise up drastically in flux at 250 GHz. To eliminate this problem, we averaged all 250 GHz flux measurements on these flat spectrum sources. As the time scales of the flares tend to be smaller than the 3 year baseline of the observations, the extreme spectral indices were brought more in line.

On the other hand, inverted spectral indices will be seen, and there will be some previously "unknown" sources popping up at 0.5-1.0 Jy at 250 GHz, so the inclusion of highly inverted sources is somewhat justified. Note that J0010+110 has an average CLASS 8.4 GHz flux of 245 mJy, which would lead to a highly inverted spectrum of -0.63. More recent observations by Barvainis *et al.* show the 8.4 GHz flux rising from 42 mJy to 750 mJy between 1997 and 1999. Because of the extreme nature of this source, and the fact that it's highly inverted spectral index could have a major impact on the estimated 250 GHz source counts, we omit it from the spectral index distribution.

Now consider the sources with $\alpha > 0.8$. A couple of detections show $\alpha \simeq 1.1$, and one source which was not detected at 250 GHz is steeper than 1.3. Nine out of the 25 sources with $\alpha > 0.8$ were not detected at 250 GHz. However, it is significant that we have good solid 250 GHz detections which define the overall shape of the spectral index distribution at the steep end. This fact permits us to use the spectral index distribution of the detected sources to statistically infer the spectral index distribution of the non-detected sources, as all but one lie within the bounds of the distribution of the detected sources. The astro-statistical program *asurv* (Feigelson and Nelson, 1985) implements a survival technique, the Kaplan-Meier algorithm, to treat the lower limit α values in estimating the spectral index distribution[1]. Including the lower limits in the distribution estimation results in a modest steepening of the spectral index distribution, which will result in fewer sources in our estimated counts at 250 GHz. Hence, using the non-detections at 250 GHz is the conservative thing to do.

The spectral index distribution between 8.4 GHz and 250 GHz derived from *asurv* is shown in solid line in Figure 3. The most-likely model for the spectral index distribution between 8.4 GHz and 250 GHz from Holdaway and Owen (2005) is shown as a dashed line. The distribution derived from the 250 GHz data has more flat and inverted spectrum sources than the Holdaway and Owen estimate, and so it implies more sources at 250 GHz. Note that this spectral index distribution will not be an intrinsic distribution, but is broadened by variability, but this is still a valid spectral index distribution to use for source count estimates.

2.4 Scaling up to 250 GHz

It is straightforward to use the spectral index distribution found in the previous section to estimate the 250 GHz source counts. The spectral index distribution is applied to the cores-only 5 GHz flat spectrum source counts. Most sources go down in flux. The few sources with inverted spectra go up in flux. On balance, as we go to higher frequencies we have fewer sources. We show our estimated source counts at 250 GHz in Figure 4 as a solid line. For comparison, we have also included the estimated counts at 250 GHz from Holdaway and Owen (2005). At 10 mJy, the current estimated counts exceed the extrapolation of Holdaway and Owen by 14%. At 100 mJy, the current estimate is 33% higher, and at 1 Jy, the current estimate is 55% higher. All in all, this is excellent agreement considering Holdaway and Owen had no actual data above 90 GHz.

[1]Note that *asurv* is no longer a supported system. Even though the code is available over the internet, it does not compile on Linux systems because of name space issues and a call to the subroutine which implements the Buckley-James method which is frankly in error and probably never worked. As the Buckley-James method is not required for the Kaplan-Meier algorithm, we just deleted that code from our copy of *asurv* to permit compiling.

3 Discussion

3.1 Intrinsic Spectral Index or High Frequency Variability?

The 8 GHz fluxes were measured with the VLA in the 1990's, and the 250 GHz fluxes were measured with MAMBO between 2002 and 2005. As such, the spectral index distribution we derive will reflect both intrinsic spectral variations and frequency dependent source variability. At 5 GHz, most sources will have relatively modest variability (J0010+110 being one marked exception). Anyway, at 5 GHz, the flat spectrum sources will always be flickering up and down a bit, but the statistical properties of the ensemble of flat spectrum sources should remain essentially constant, especially at lower flux levels where there are more sources. The 8 GHz flat spectrum source fluxes will show a bit more variability, but again the statistical properties of the source counts should remain fairly constant. However, at 250 GHz, the source fluxes are jumping around quite a bit. As mentioned earlier, we have chosen to average all 250 GHz flux measurements to dampen out some of this high frequency variability.

However, the change in spectral index due to the measured variability at 250 GHz is small compared to the source's intrinsic spectral index distribution. The median percent variability is 20%, which leads to a change in $\alpha_{8.4}^{90}$ of 0.054. The third quartile percent variability is at the 32% level, which leads to a change in $\alpha_{8.4}^{90}$ of 0.082. The 90% value of the percent variability is 49% (ie, only 10% of our sources are more variable than 49%), leading to a change in $\alpha_{8.4}^{90}$ of 0.12. Meanwhile, the spectral index distribution ranges from -0.5 to 1.3. While variability will lead to some broadening of the spectral index distribution, it is a relatively minor effect. Statistically, the results we get by measuring the spectral index distribution will be similar, whether we measure the 8.4 GHz and 250 GHz fluxes simultaneously or in different decades, as long as the flaring among the different sources is not correlated through some unfortunate selection effect.

The inverted members of the spectral index distribution are real, and there will be sources such as J0010+110 which will not be well known at centimeter wavelengths, but will be very bright at millimeter wavelengths for a time. There may be only a few such sources in the sky at the 0.5-1 Jy level at any given time, but there will be hundreds at the 100 mJy level, and thousands at the 30 mJy level. These sources could be an important sub-population of the fast switching phase calibrators. Of course, the trick is to find these sources.

3.2 Where Are All The Sources at High Frequencies?

Several people have bemoaned within earshot that there just aren't as many sources at high frequencies as claimed by HOR or Holdaway and Owen. And now in this memo, we are saying there are even *more* sources at 250 GHz than predicted by Holdaway and Owen. So far, these criticisms of the source count work have been anecdotal or qualitative. We look forward to more quantitative comparisons.

It seems that one possible shortcoming to this work is that the Patnaik-type sources observed with MAMBO may be only a sub-population of the 5 GHz flat spectrum source counts, and applying their spectral index distribution to the full 5 GHz flat spectrum source counts is therefore not appropriate. However, the Patnaik sources were drawn from 1.4 GHz and 5 GHz single dish flux measurements and the requirement that the spectral index be flat ($\alpha < 0.5$), precisely the selection criteria for the 5 GHz flat spectrum counts which we base our analysis upon.

Another possible shortcoming is that the 3CR2 quasars sub-sample's core fraction distribution does not adequately reflect the core fraction of the weaker sources which make up the 5 GHz flat spectrum counts. In order for this to affect our count estimates, the weaker flat spectrum sources would need to have significantly more extended steep spectrum emission than their bright flat spectrum 3CR2 counterparts.

On the other side of the argument, Voss *et al.* (*in press*, 2005) have discovered a significant overabundance of quasars in 2200 square arcminute blank field observations at 250 GHz. Three non-thermal sources brighter than 10 mJy were discovered in the blank fields, roughly 8 times more than expected by the model of Holdaway and Owen.

We look forward to opportunities in the future to answer the high frequency source counts question more definitively.

3.3 Impact on Fast Switching Phase Calibration

There are two different flavors of fast switching: a) calibration observations being done at 90 GHz and target observations at a higher frequency, and b) calibration observations being done at the target frequency. If the calibration and target frequency are different, we need to perform a second calibration every 5-10 minutes to track the non-common mode instrumental drifts across the two bands, which will reduce the efficiency of the calibration observations. If the cal and target frequencies are the same, we save by not having to perform this extra instrumental calibration, but at very high frequencies we will lose big as the calibrators become weaker and the ALMA sensitivity becomes worse. In earlier work (LAMA Memo 803), we found that at about 350 GHz and below, it is more efficient to calibrate at the target frequency, but above 350 GHz it is more efficient to calibrate at 90 GHz, scale the calibrator phases up to the target frequency, and track the non-common mode dual band instrumental phase shifts. As the current work indicates that there may be more bright sources at high frequencies than our earlier calculations had assumed, this will tend to make calibrating at the target frequency more efficient, and the target frequency above which we perform the calibration at 90 GHz could rise. Increased efficiency of the cross-band instrumental calibration will be a second order effect. We plan to reevaluate fast switching in light of these new source count estimates in advance of the 2006 URSI meeting.

4 References

Barvainis *et al.*, 2005, "Radio Variability of Radio-quiet and Radio-loud Quasars", **ApJ**, 618, 108.

Condon, 1984, "Cosmological Evolution of Radio Sources", **ApJ**, 287, 461.

Feigelson, E.D., and P.J. Nelson, 1985, **ApJ**, 293, 192.

Holdaway, M.A., and F.N. Owen 2005, "A Refined Method for Estimating Calibrator Counts Above 90 GHz", ALMA Memo 520.

Holdaway, M.A., F.N. Owen, and M.P. Rupen, 1994, "Source Counts at 90 GHz", ALMA Memo 123.

Myers, S.T., et al., 2003, **MNRAS**, 341, 1-12.

Patnaik et al, 1993, **MNRAS** 261, 435.

Voss, H., *et al.*, "Quasars in the MAMBO blank field survey", *in press* **A&A**, astro-ph/0511117, 2005.

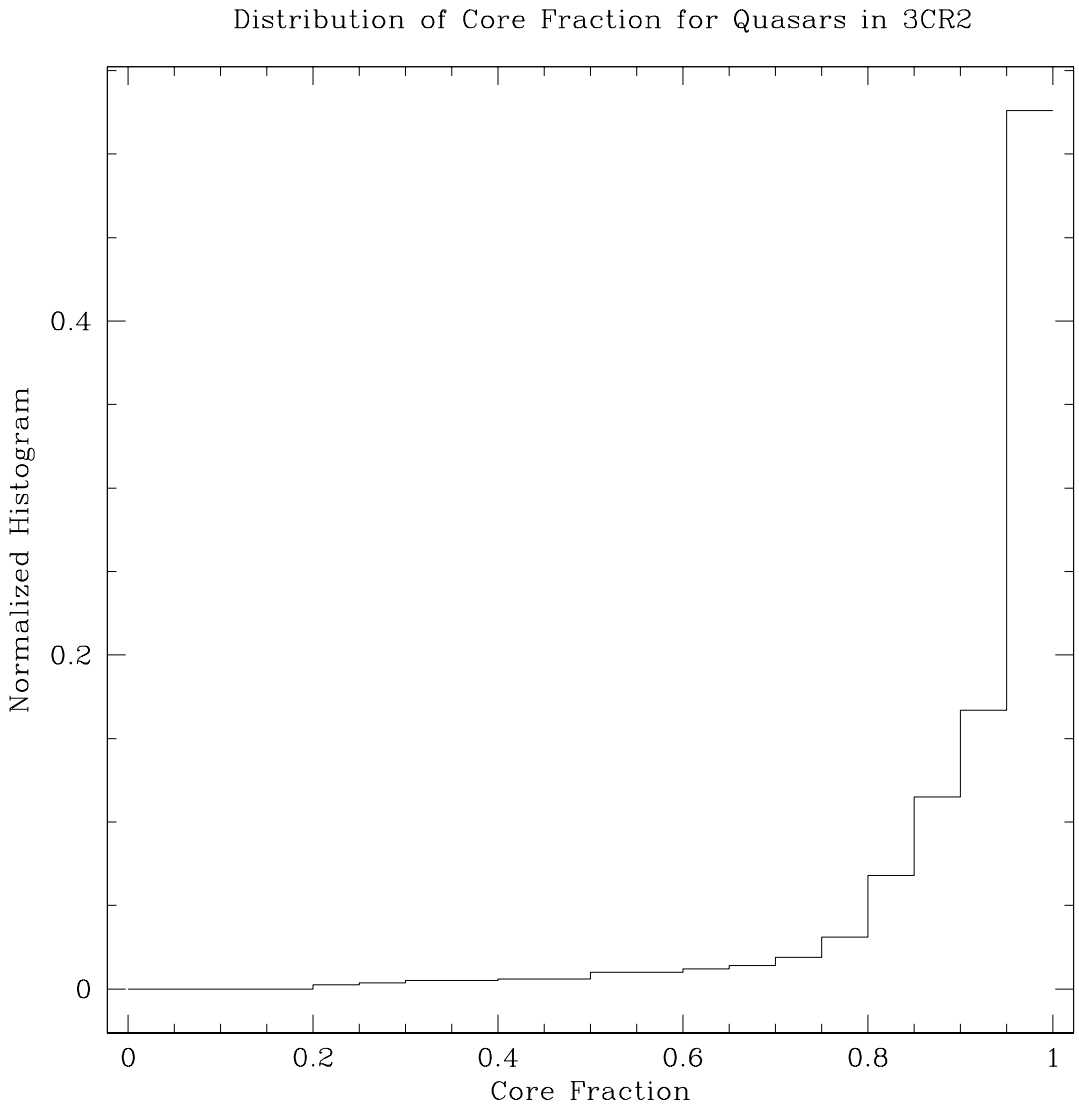

Figure 1: The distribution of core fraction derived from the quasar members of the 3CR2 catalog (ie, neglecting radio galaxies, which will be steep spectrum objects).

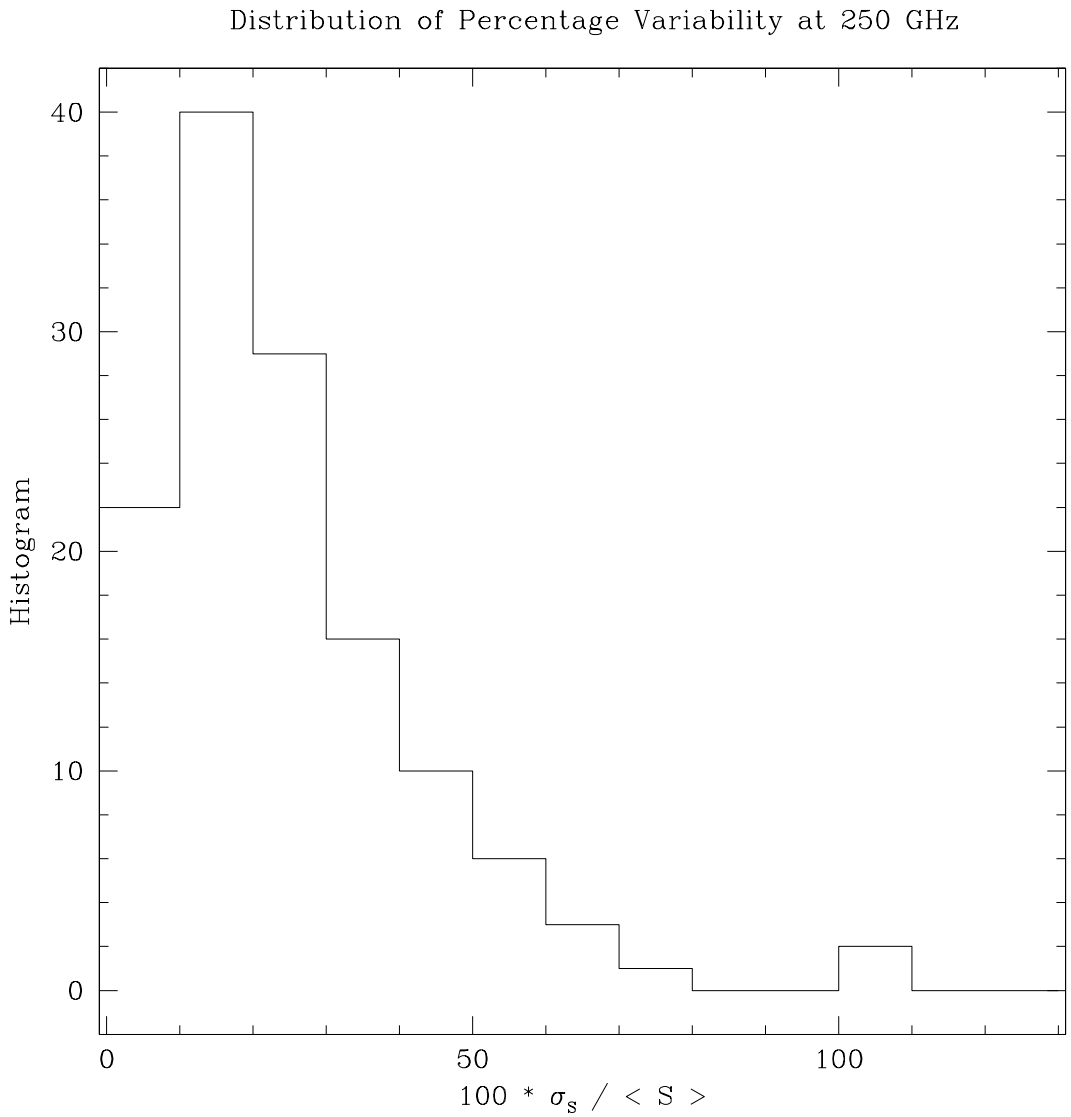

Figure 2: Histogram of the percent variability at 250 GHz derived from all sources which have been observed with MAMBO more than once.

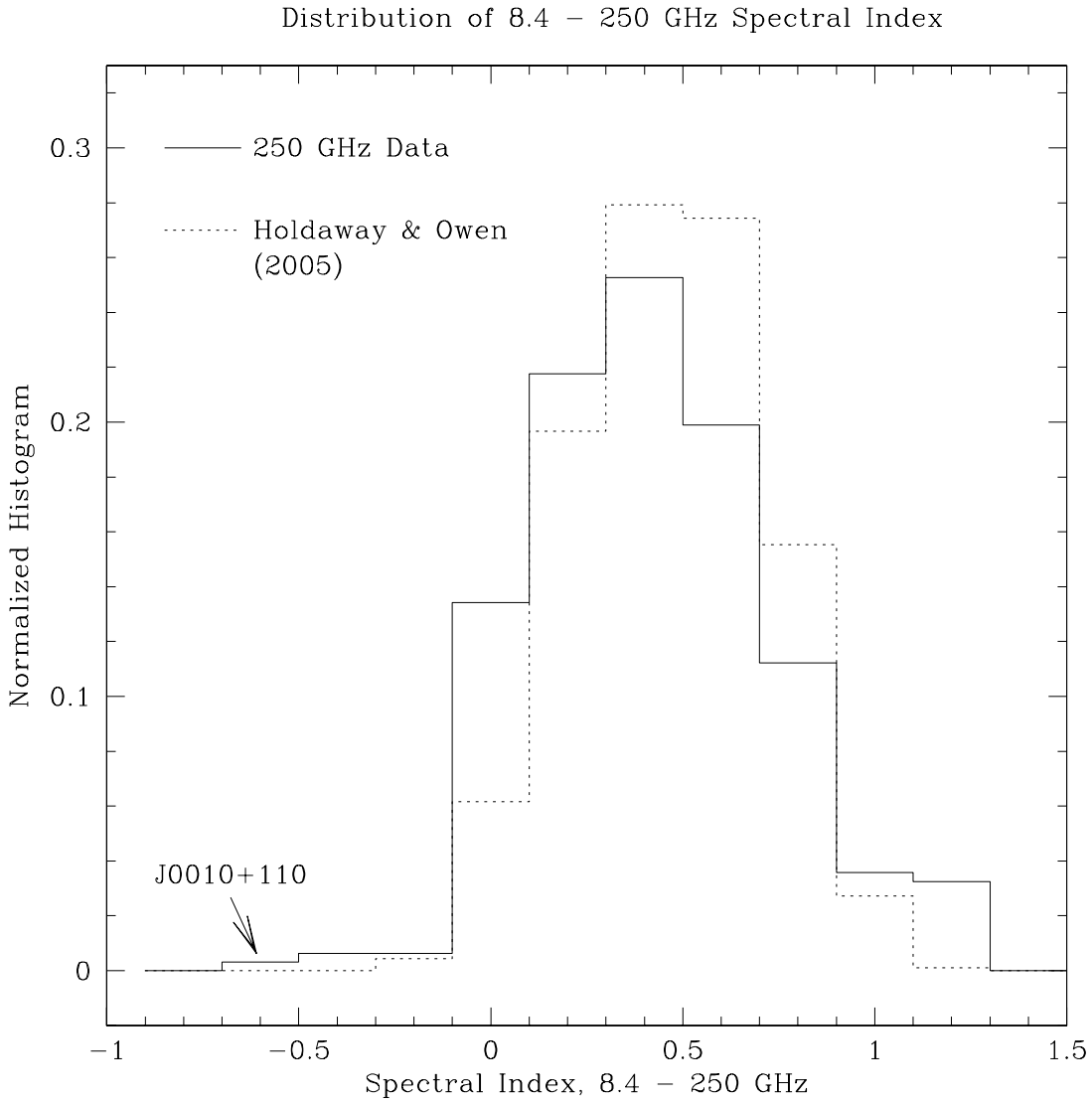

Figure 3: The distribution of spectral index between 8.4 and 250 GHz ($S(\nu) \propto \nu^{-\alpha}$) using Feigelson's *asurv* package to handle sources not detected at 250 GHz. Of 313 sources, 12% were below the 20 mJy detection threshold at 250 GHz, 64% are still "flat spectrum sources" by the definition of $\alpha < 0.5$, and 9% are still inverted even at 250 GHz. There are two notable mm-flaring sources in this database: J2253+161, (3C454.3), which had a spectral index of -0.38, and J0010+110, which had a spectral index of -0.72. J2253+161 was left in for the *asurv* distribution, though it increases the source counts by only a few percent. J0010+110 was censored as an outlier for the spectral index distribution determination. If this source were included, the estimated source counts would have increased by over 10%.

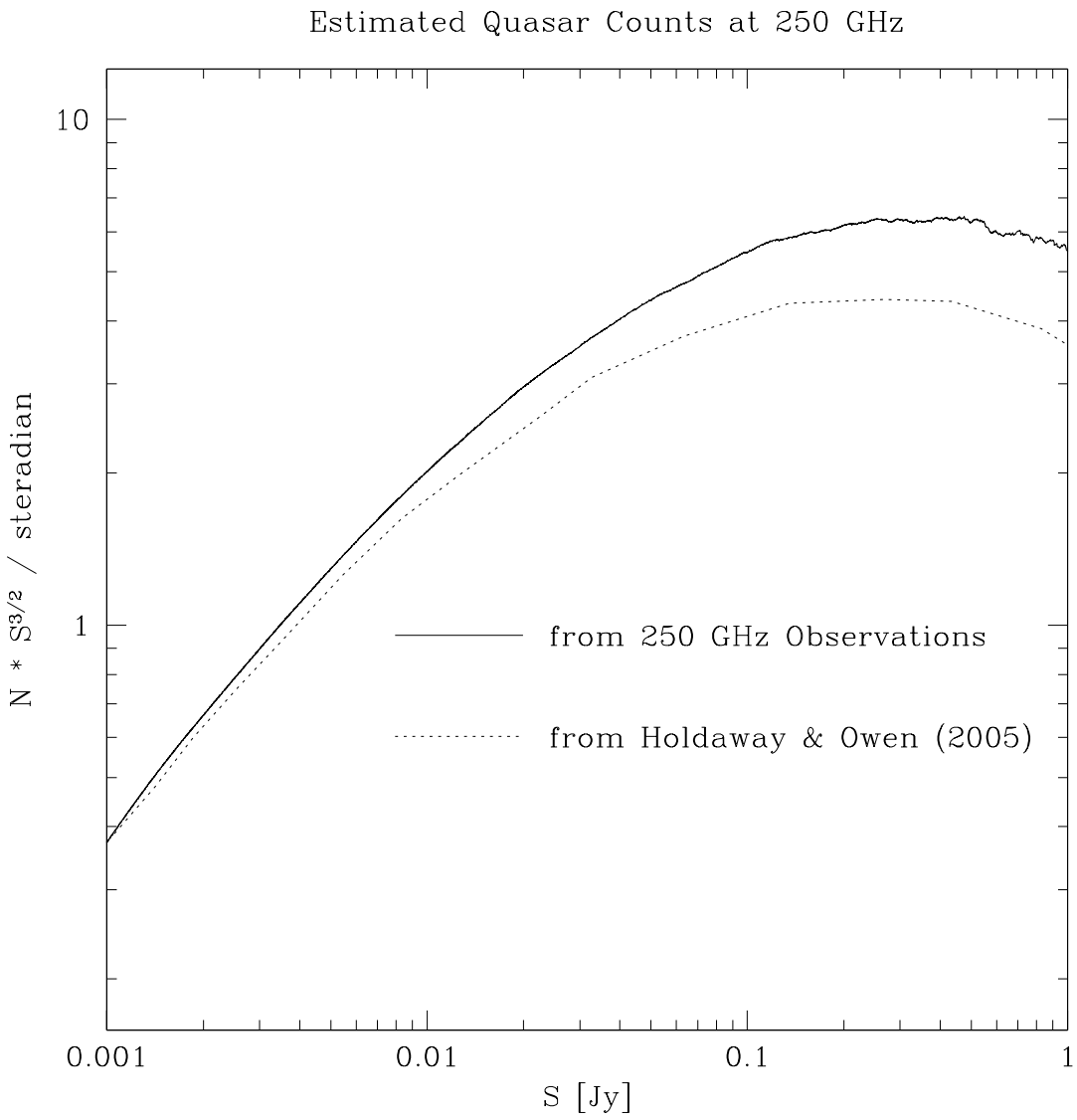

Figure 4: Estimated integral source counts at 250 GHz. The solid line indicates the counts inferred from the 8.4 - 250 GHz spectral index distribution determined from *asurv*, neglecting the flaring source J0010+110, which appears highly inverted. The lower dotted line indicates the 250 GHz counts expected from the model of Holdaway and Owen (2005), which is based upon 90 GHz measurements and an assumed distribution of break frequencies, above which the spectral index becomes approximately 0.8.

Source Name	Flux at 8.4 GHz [mJy]	Flux at 250 GHz [mJy]	α	Lower Limit to α
J0004+203	162.5	150.5	0.0223	0
J0005+383	1077.6	369.1	0.3113	0
J0005+545	382.4	473.0	-0.0618	0
J0006+244	230.9	20.0	0.7107	1
J0010+110	245.0	2128.0	-0.6280	0
J0010+208	272.1	61.3	0.4330	0
J0013+409	546.4	351.9	0.1278	0
J0019+204	1232.9	44.0	0.9683	0
J0019+735	1330.7	734.7	0.1726	0
J0023+449	240.0	20.0	0.7219	1
J0025+393	485.9	43.1	0.7038	0
J0038+416	1009.3	48.0	0.8849	0
J0039+490	298.2	20.0	0.7850	1
J0042+571	895.3	214.0	0.4158	0
J0048+320	286.2	304.5	-0.0180	0
J0049+515	226.3	45.0	0.4693	0
J0057+304	687.0	76.0	0.6396	0
J0102+584	1426.8	1158.2	0.0606	0
J0106+340	321.2	74.5	0.4245	0
J0108+016	2263.2	559.4	0.4060	0
J0112+227	493.4	548.9	-0.0310	0
J0121+044	1351.7	214.0	0.5355	0
J0122+299	160.1	85.8	0.1814	0
J0130+087	264.4	119.6	0.2305	0
J0136+479	1644.0	1746.6	-0.0176	0
J0143+123	96.7	20.0	0.4578	1
J0148+389	350.8	36.9	0.6543	0
J0151+549	152.2	50.0	0.3234	0
J0152+373	266.6	52.1	0.4743	0
J0204+152	3325.0	257.0	0.7438	0

Table 1: Sources, source flux at 8.4 GHz and 250 GHz, and derived spectral index or lower limit of the spectral index in the event the 250 GHz flux is below the 3 sigma level of 20 mJy. The "lower limit to α" flag is due to nondetections at 250 GHz.

Source Name	Flux at 8.4 GHz [mJy]	Flux at 250 GHz [mJy]	α	Lower Limit?
J0217+017	1178.9	407.8	0.3084	0
J0217+738	2292.8	675.2	0.3552	0
J0224+070	826.5	375.9	0.2289	0
J0228+674	1806.2	309.4	0.5126	0
J0230+405	581.1	191.1	0.3230	0
J0237+288	3123.0	1861.1	0.1504	0
J0238+166	5453.5	1143.9	0.4537	0
J0258+057	243.6	93.3	0.2788	0
J0259+078	456.3	128.5	0.3681	0
J0301+060	318.8	29.6	0.6905	0
J0303+473	1616.3	336.4	0.4560	0
J0305+054	200.7	20.0	0.6700	1
J0313+025	130.6	121.8	0.0203	0
J0319+415	34295.6	2295.7	0.7856	0
J0321+065	90.2	20.0	0.4376	1
J0323+048	112.6	20.0	0.5021	1
J0336+323	1238.3	554.4	0.2335	0
J0339-018	2425.4	735.4	0.3467	0
J0359+510	2454.1	2886.5	-0.0472	0
J0403+260	786.4	187.4	0.4167	0
J0414+343	1314.6	53.0	0.9329	0
J0423-013	4120.1	5919.0	-0.1053	0
J0429+274	353.9	32.1	0.6973	0
J0433+054	2105.2	1587.5	0.0820	0
J0433+291	432.8	140.9	0.3261	0
J0435+255	217.4	31.9	0.5576	0
J0438+301	572.0	50.0	0.7080	0
J0439+308	303.1	27.0	0.7026	0
J0440+275	222.0	20.0	0.6993	1
J0459+025	1265.4	25.6	1.1332	0

Table 2: Sources, source flux at 8.4 GHz and 250 GHz, and derived spectral index or lower limit of the spectral index in the event the 250 GHz flux is below the 3 sigma level of 20 mJy.

Source Name	Flux at 8.4 GHz [mJy]	Flux at 250 GHz [mJy]	α	Lower Limit?
J0501-020	3305.7	478.1	0.5618	0
J0503+021	1469.9	81.3	0.8410	0
J0505+050	808.5	329.2	0.2610	0
J0511+012	317.8	55.5	0.5070	0
J0513+010	344.5	27.1	0.7387	0
J0520+021	139.7	20.0	0.5647	1
J0522+012	365.1	23.7	0.7945	0
J0527+035	327.8	495.5	-0.1200	0
J0530+135	2458.2	1226.2	0.2021	0
J0532+013	113.6	528.1	-0.4464	0
J0532+075	2763.4	411.0	0.5536	0
J0533+484	556.9	638.7	-0.0398	0
J0547+274	273.8	133.4	0.2089	0
J0552+192	158.5	159.5	-0.0018	0
J0555+398	7428.6	483.8	0.7936	0
J0558+343	146.1	84.8	0.1580	0
J0604+442	454.4	42.0	0.6918	0
J0607+477	403.4	150.2	0.2870	0
J0607+673	598.8	64.1	0.6492	0
J0610+728	409.4	29.5	0.7642	0
J0615+483	241.8	20.0	0.7241	1
J0623+227	297.3	46.3	0.5403	0
J0624+389	642.0	65.1	0.6649	0
J0630+176	217.4	29.5	0.5803	0
J0632+159	103.3	35.0	0.3144	0
J0633+367	156.1	62.2	0.2673	0
J0638+250	124.0	33.1	0.3837	0
J0638+596	575.6	63.4	0.6409	0
J0642+352	188.8	127.2	0.1147	0
J0646+307	378.3	20.0	0.8541	1

Table 3: Sources, source flux at 8.4 GHz and 250 GHz, and derived spectral index or lower limit of the spectral index in the event the 250 GHz flux is below the 3 sigma level of 20 mJy.

Source Name	Flux at 8.4 GHz [mJy]	Flux at 250 GHz [mJy]	α	Lower Limit?
J0646+449	2258.4	439.7	0.4754	0
J0657+244	360.1	149.0	0.2564	0
J0707+612	230.8	56.7	0.4078	0
J0710+475	620.1	216.3	0.3060	0
J0717+456	562.4	203.9	0.2948	0
J0719+331	176.1	180.3	-0.0068	0
J0720+476	248.7	78.1	0.3365	0
J0721+713	594.8	1906.8	-0.3384	0
J0728+570	644.3	32.7	0.8660	0
J0735+478	460.5	30.6	0.7877	0
J0737+597	248.3	20.0	0.7318	1
J0738+177	3738.2	513.2	0.5769	0
J0739+016	1710.8	2095.3	-0.0589	0
J0742+547	142.8	20.0	0.5711	1
J0743+397	316.8	25.2	0.7354	0
J0748+240	1541.6	460.5	0.3510	0
J0749+743	398.6	77.7	0.4750	0
J0750+792	167.9	42.8	0.3971	0
J0750+827	676.9	41.1	0.8139	0
J0751+332	423.8	68.3	0.5303	0
J0753+539	1196.9	338.9	0.3665	0
J0757+099	1363.5	574.9	0.2509	0
J0808+010	136.7	20.0	0.5584	1
J0808+409	1181.8	181.1	0.5450	0
J0808+498	880.0	225.9	0.3951	0
J0809+349	152.1	29.2	0.4795	0
J0811+018	1284.6	401.5	0.3379	0
J0811+572	356.5	75.8	0.4498	0
J0814+645	221.6	51.6	0.4234	0
J0817+325	361.1	49.9	0.5750	0

Table 4: Sources, source flux at 8.4 GHz and 250 GHz, and derived spectral index or lower limit of the spectral index in the event the 250 GHz flux is below the 3 sigma level of 20 mJy.

Source Name	Flux at 8.4 GHz [mJy]	Flux at 250 GHz [mJy]	α	Lower Limit?
J0818+424	1041.2	315.0	0.3474	0
J0819+324	272.8	145.9	0.1818	0
J0821+290	155.7	57.4	0.2899	0
J0823+295	374.3	59.7	0.5333	0
J0824+559	1736.1	109.1	0.8038	0
J0825+032	1873.4	1448.6	0.0747	0
J0825+135	241.2	81.6	0.3149	0
J0825+620	628.0	28.5	0.8985	0
J0834+603	349.7	21.9	0.8049	0
J0841+709	1752.1	582.3	0.3201	0
J0852+286	215.6	152.9	0.0999	0
J0854+201	3414.9	2566.8	0.0829	0
J0902+432	363.4	20.0	0.8425	1
J0904+426	389.9	88.0	0.4325	0
J0905+288	255.6	48.0	0.4859	0
J0909+014	765.8	1070.6	-0.0973	0
J0911+338	278.7	64.0	0.4274	0
J0912+221	181.2	99.0	0.1756	0
J0916+389	483.5	207.0	0.2465	0
J0919+334	333.2	71.0	0.4492	0
J0920+447	1368.3	547.4	0.2662	0
J0923+283	218.4	281.3	-0.0735	0
J0923+311	167.5	22.0	0.5898	0
J0923+388	375.7	99.0	0.3875	0
J0925+315	289.6	60.0	0.4573	0
J0927+390	9176.5	1405.9	0.5450	0
J0929+731	167.6	20.3	0.6133	0
J0930+351	460.0	104.0	0.4320	0
J0932+337	156.9	30.0	0.4807	0
J0937+501	372.5	268.5	0.0951	0

Table 5: Sources, source flux at 8.4 GHz and 250 GHz, and derived spectral index or lower limit of the spectral index in the event the 250 GHz flux is below the 3 sigma level of 20 mJy.

Source Name	Flux at 8.4 GHz [mJy]	Flux at 250 GHz [mJy]	α	Lower Limit?
J0939+417	277.8	32.0	0.6279	0
J0940+261	442.9	177.0	0.2665	0
J0945+356	273.1	26.0	0.6832	0
J0948+004	226.8	253.1	-0.0319	0
J0948+407	1323.2	252.1	0.4817	0
J0952+352	319.6	44.0	0.5761	0
J0956+253	1786.8	183.4	0.6613	0
J0957+554	1498.9	189.3	0.6011	0
J0958+474	879.6	355.5	0.2632	0
J0958+656	1247.2	939.3	0.0824	0
J1001+292	296.0	297.8	-0.0018	0
J1011+011	195.8	20.8	0.6514	0
J1015+012	163.1	20.1	0.6083	0
J1016+206	1017.7	64.0	0.8037	0
J1017+613	582.7	32.5	0.8386	0
J1019+633	272.7	119.3	0.2401	0
J1024+192	642.8	20.0	1.0082	1
J1031+603	283.5	330.5	-0.0446	0
J1033+072	203.3	40.0	0.4723	0
J1033+413	384.4	216.7	0.1665	0
J1033+609	430.4	181.1	0.2516	0
J1038+427	165.6	84.0	0.1972	0
J1043+241	685.4	465.5	0.1124	0
J1044+809	1020.8	88.5	0.7104	0
J1048+717	1284.5	876.0	0.1112	0
J1056+702	607.2	277.8	0.2271	0
J1058+016	3582.0	1901.2	0.1840	0
J1058+431	232.9	87.0	0.2861	0
J1058+565	189.8	64.0	0.3158	0
J1058+812	571.4	396.0	0.1065	0

Table 6: Sources, source flux at 8.4 GHz and 250 GHz, and derived spectral index or lower limit of the spectral index in the event the 250 GHz flux is below the 3 sigma level of 20 mJy.

Source Name	Flux at 8.4 GHz [mJy]	Flux at 250 GHz [mJy]	α	Lower Limit?
J1101+724	366.7	67.3	0.4926	0
J1101+724	631.6	198.7	0.3360	0
J1104+606	181.2	73.0	0.2641	0
J1108+435	288.0	151.2	0.1873	0
J1118+126	266.4	39.0	0.5582	0
J1118+126	1577.0	279.4	0.5028	0
J1125+262	992.6	160.1	0.5301	0
J1127+568	497.7	47.0	0.6856	0
J1146+400	575.7	539.1	0.0191	0
J1159+292	1233.3	691.3	0.1682	0
J1209+182	136.3	143.7	-0.0154	0
J1211+183	273.8	41.6	0.5474	0
J1213+131	276.1	40.0	0.5613	0
J1215+169	400.1	257.3	0.1283	0
J1215+175	244.2	20.0	0.7270	1
J1229+021	41725.0	4490.5	0.6476	0
J1250+137	156.6	20.0	0.5979	1
J1300+085	128.9	31.4	0.4103	0
J1306+112	63.8	20.0	0.3370	1
J1309+119	785.1	270.0	0.3101	0
J1310+323	3061.0	997.3	0.3258	0
J1310+326	620.6	185.8	0.3505	0
J1315+123	192.7	45.2	0.4213	0
J1331+061	190.5	20.0	0.6548	1
J1334+092	120.9	63.5	0.1871	0
J1357+193	1130.5	729.0	0.1275	0
J1400+044	155.6	20.0	0.5960	1
J1404-002	436.2	50.8	0.6247	0
J1405+043	868.0	120.8	0.5731	0
J1410+075	335.1	56.0	0.5198	0

Table 7: Sources, source flux at 8.4 GHz and 250 GHz, and derived spectral index or lower limit of the spectral index in the event the 250 GHz flux is below the 3 sigma level of 20 mJy.

Source Name	Flux at 8.4 GHz [mJy]	Flux at 250 GHz [mJy]	α	Lower Limit?
J1415+133	1564.3	462.9	0.3538	0
J1419+384	775.8	263.9	0.3133	0
J1419+544	2248.1	661.4	0.3555	0
J1420+068	44.7	20.0	0.2337	1
J1422+324	527.9	83.6	0.5354	0
J1424+046	145.7	55.0	0.2830	0
J1435+302	309.0	30.8	0.6699	0
J1439+500	244.6	268.8	-0.0274	0
J1442+326	342.6	20.0	0.8253	1
J1500+479	678.0	123.0	0.4959	0
J1504+105	1686.8	266.7	0.5359	0
J1506+375	948.8	72.0	0.7491	0
J1506+427	412.6	284.0	0.1085	0
J1531+721	232.5	32.6	0.5708	0
J1539+277	291.5	95.6	0.3238	0
J1549+026	918.7	1221.7	-0.0828	0
J1550+055	1614.6	812.2	0.1996	0
J1606+273	216.3	84.1	0.2744	0
J1608+105	1784.0	776.2	0.2418	0
J1610+242	405.1	69.6	0.5117	0
J1613+342	3088.1	1104.7	0.2987	0
J1619+228	649.5	21.0	0.9970	0
J1635+381	2413.3	1604.7	0.1186	0
J1637+473	766.7	354.2	0.2243	0
J1638+573	1338.2	995.7	0.0859	0
J1640+398	1650.8	156.0	0.6854	0
J1642+254	237.9	126.3	0.1840	0
J1642+398	6299.8	1981.9	0.3360	0
J1642+689	1206.2	711.9	0.1532	0
J1707+135	458.8	44.4	0.6785	0

Table 8: Sources, source flux at 8.4 GHz and 250 GHz, and derived spectral index or lower limit of the spectral index in the event the 250 GHz flux is below the 3 sigma level of 20 mJy.

Source Name	Flux at 8.4 GHz [mJy]	Flux at 250 GHz [mJy]	α	Lower Limit?
J1716+686	819.7	340.6	0.2552	0
J1728+123	365.0	236.1	0.1266	0
J1734+094	522.6	20.0	0.9480	1
J1734+390	1160.0	442.0	0.2803	0
J1735+081	296.3	77.4	0.3900	0
J1740+522	1347.2	331.6	0.4072	0
J1751+097	2015.2	1843.4	0.0259	0
J1800+785	2874.0	700.5	0.4101	0
J1801+441	522.0	594.5	-0.0378	0
J1806+698	1595.5	1014.0	0.1317	0
J1824+569	1193.1	1050.6	0.0369	0
J1842+682	846.7	345.0	0.2608	0
J1902+320	1719.3	181.1	0.6538	0
J1908+224	202.0	65.7	0.3263	0
J1919+063	100.4	77.7	0.0745	0
J1920+269	198.1	20.3	0.6619	0
J1922+087	106.0	52.2	0.2058	0
J1925+211	1414.7	571.4	0.2634	0
J1927+613	514.0	370.8	0.0948	0
J1927+740	3697.8	746.6	0.4648	0
J1935+205	505.3	79.2	0.5384	0
J1937+125	87.5	20.0	0.4288	1
J1938+048	340.2	81.7	0.4144	0
J1939+372	351.2	27.3	0.7421	0
J1947+128	243.9	20.0	0.7266	1
J1951+575	316.6	40.5	0.5974	0
J1953+356	628.0	62.5	0.6704	0
J1955+515	1822.6	356.0	0.4745	0
J1959+651	222.8	55.0	0.4064	0
J2002+069	135.2	20.0	0.5552	1

Table 9: Sources, source flux at 8.4 GHz and 250 GHz, and derived spectral index or lower limit of the spectral index in the event the 250 GHz flux is below the 3 sigma level of 20 mJy.

Source Name	Flux at 8.4 GHz [mJy]	Flux at 250 GHz [mJy]	α	Lower Limit?
J2002+451	493.7	340.6	0.2552	0
J2005+779	2674.8	236.1	0.1266	0
J2006+644	958.0	20.0	0.9480	1
J2007+066	287.7	442.0	0.2803	0
J2007+405	3247.0	77.4	0.3900	0
J2007+661	480.9	331.6	0.4072	0
J2009+725	791.9	1843.4	0.0259	0
J2012+465	587.2	700.5	0.4101	0
J2024+005	117.1	594.5	-0.0378	0
J2025+033	381.8	1014.0	0.1317	0
J2027+122	126.0	1050.6	0.0369	0
J2031+027	153.3	345.0	0.2608	0
J2038+513	4289.4	181.1	0.6538	0
J2055+614	304.3	65.7	0.3263	0
J2101+037	785.7	77.7	0.0745	0
J2106+216	294.7	20.3	0.6619	0
J2123+056	1426.3	52.2	0.2058	0
J2136+007	6725.4	571.4	0.2634	0
J2139+144	2237.5	370.8	0.0948	0
J2148+070	7026.8	746.6	0.4648	0
J2200+216	235.5	79.2	0.5384	0
J2202+423	3321.9	20.0	0.4288	1
J2203+318	2969.3	81.7	0.4144	0
J2223+628	196.1	27.3	0.7421	0
J2232+117	2923.8	20.0	0.7266	1
J2236+285	2074.2	40.5	0.5974	0
J2238+278	178.9	62.5	0.6704	0
J2241+413	825.6	356.0	0.4745	0
J2244+410	228.2	55.0	0.4064	0
J2250+558	405.4	20.0	0.5552	1

Table 10: Sources, source flux at 8.4 GHz and 250 GHz, and derived spectral index or lower limit of the spectral index in the event the 250 GHz flux is below the 3 sigma level of 20 mJy.

Source Name	Flux at 8.4 GHz [mJy]	Flux at 250 GHz [mJy]	α	Lower Limit?
J2251+405	137.9	75.0	0.1769	0
J2253+161	10380.1	12864.9	-0.0624	0
J2301+374	361.8	290.5	0.0638	0
J2311+457	614.3	20.0	0.9950	1
J2312+727	217.4	69.7	0.3305	0
J2320+052	368.5	178.7	0.2102	0
J2321+275	505.9	560.2	-0.0296	0
J2322+448	347.0	22.8	0.7910	0
J2322+510	1676.8	20.0	1.2867	1
J2340+267	711.1	20.0	1.0375	1
J2343+237	442.7	228.2	0.1925	0
J2354+459	990.9	403.9	0.2607	0
J2356+819	517.3	163.8	0.3341	0

Table 11: Sources, source flux at 8.4 GHz and 250 GHz, and derived spectral index or lower limit of the spectral index in the event the 250 GHz flux is below the 3 sigma level of 20 mJy.